Engineered Science
DOI: https://dx.doi.org/10.30919/es1559

Integrated Thermal Conversion of Petroleum Residues and Waste Engine Oils for Enhanced Coke Production

Yermek Aubakirov* and Kainaubek Toshtay*

Abstract

Heavy oil residues are significant waste streams in the petroleum refining industry, although delayed coking stands out as a promising method for its processing, which allows the use of a wider range of other raw materials. This article discusses an approach to adding waste engine oils in delayed coking processes. The influence of petroleum residues (tar) and temperature on the quality and yield of target products, such as liquid hydrocarbons and solid residue - petroleum coke, is analyzed. The change patterns in the composition, properties and structure of products were determined by gas chromatography, Raman and infrared spectroscopy, scanning electron microscopy and Brunauer-Emmett-Teller method. The results have shown that the analyzed coke has decent ash, metallic, moist and volatile matter contents. Therefore, it can be used in the production of anodes. The structure of coke obtained from tar in the presence of engine oils corresponds to needle coke. The product yield exhibited a temperature-dependent behavior, with higher temperatures promoting increased formation of coke and gaseous products. In order to obtain efficient product yield and coke with decent structure and porosity, with residual engine oils, it is necessary to conduct coking at a temperature of 500 °C.

Keywords: Coke; Pyrolysis; Petroleum residues; Waste engine oils; Liquid product.
Received: 25 April 2025; Revised: 20 May 2025; Accepted: 21 May 2025.
Article type: Research article.

1. Introduction

Coking is a critical phenomenon that can impact the efficiency and longevity of equipment during various manufacturing processes. It typically involves the unwanted deposition of carbonaceous materials on surfaces exposed to high temperatures. In industrial settings, coking occurs through three distinct methods, each influenced by specific operating conditions and material characteristics. In the operation of the delayed coking unit, fine coke with a particle size of up to 0.3 mm is used. Coke formation takes place on a fluidized bed within a heat exchanger. Separation of coke from the heat exchanger is achieved through pneumatic conveying, primarily driven by steam and gas flows. These carriers facilitate the removal of coke particles from the system.[1-5]

Three processes simultaneously occur on the fluidized bed in the process of delayed coking: the coking process with the formation of compaction and decomposition products, the secondary reactions of the compaction and decomposition products in the gas phase, and coke passing through with the release of light products from coke. Coke in the heater helps evaporate the products and separate them from the surface of the coke particles.[6-9] Reduces the ability to recreate products using this process. Therefore, the coke yield may be less in delayed coking than in normal coking.

At lower temperatures, the slow rate of cracking reactions results in the predominance of naphthenic-aromatic structures with short alkyl chains in the product mixture,[10,11] which hinders subsequent condensation reactions. At temperatures above the optimum, the rates of both cracking and polycondensation reactions increase significantly. Therefore, to enhance the yield of liquid coking products, it is advisable to operate the process at elevated temperatures, which promotes the formation of naphthenic-aromatic compounds with short alkyl chains, as well as normal olefins formed via thermal cracking.[11-13] Increasing the feedstock heating temperature intensifies hydrocarbon cracking reactions, leading to higher gas yields, reduced coke formation, and a redistribution of gasoline and diesel-range coking fractions.[12-16]

Gas yield is highly influenced by the pressure inside the coking reactor, as evidenced by studies,[15-18] which report a significant increase in coking gas production with rising pressure. Elevated pressure in the coke oven chambers also

Al-Farabi Kazakh National University, Faculty of Chemistry and Chemical Technology, Almaty, 050040, Kazakhstan
**Email:* ermek.aubakirov@kaznu.edu.kz (Y. Aubakirov); kainaubek.toshtay@kaznu.kz (K. Toshtay)

results in a substantial increase in coke yield, accompanied by a reduction in the yield of distillate fractions.[13] Additionally, higher pressure contributes to the formation of more ordered coke structures.[5,13] The observed decrease in heavy coking gas oil yield with increasing pressure can be attributed to the higher solubility of intermediate products in the liquid phase and the condensation of polycondensation products from the vapor phase onto the surface of coke particles. This phenomenon reduces the yield of liquid products while enhancing coke formation.[11,16]

The recycle feed ratio typically ranges from 0.2 to 0.6.[14,16] An increase in the recycling coefficient (defined as the ratio of secondary to primary feedstock) results in a slight increase in coke yield relative to the total feed input.[15-17] Higher recycling coefficients also lead to increased yields of gas, gasoline, and heavy gas oil.[19] Under high-temperature and low-pressure conditions (*i.e.*, pyrolysis), significant amounts of reactive low-molecular-weight hydrocarbons are produced. The gas oil fraction derived from coking contains approximately 30–40% polycyclic aromatic hydrocarbons. Consequently, recycling this fraction enhances aromaticity, improves aggregate stability, and facilitates the formation of supramolecular structures, thereby influencing the development and quality of the resulting coke.

This research presents a novel and promising approach for producing low-sulfur coke suitable for the aluminum industry from oil tar sourced from the Kumkol field in Kazakhstan. The proposed method outlines the optimal technological conditions required to maximize the yield of light fuel fractions with a favorable chemical composition. Furthermore, the study investigates the patterns of change in the yield, composition, and properties of delayed coking products derived from Kumkol oil tars as a function of key process parameters. This approach not only facilitates the efficient production of low-sulfur coke but also addresses environmental concerns and supports the development of alternative energy sources. This study investigates the coking of heavy oil waste at atmospheric pressure within a temperature range of 500–520 °C, with the objective of analyzing the physicochemical properties of the resulting fuel distillates, characterizing the composition and microstructure of the produced coke, and evaluating its potential applications in industrial processes such as foundry operations and anode manufacturing.

2. Materials and methods

2.1 Obtain the procedure for the cooking process

The experimental setup involved catalyst-free delayed coking using a laboratory-scale reactor. A laboratory autotransformer was used to regulate the current, enabling precise control of the reactor's heating until the desired temperature was reached. Experiments were conducted at temperatures of 480, 500, and 520 °C for a duration of 3 hours. The reactor had a volume of 200 mL. Temperature monitoring and control were achieved via a thermocouple integrated into the reactor.

Initially, 12 g of petroleum residues (tar) and 8 g of residual engine oil were introduced into the reactor to initiate the coking process. The reactor was then sealed with a lid to ensure airtightness. The system was continuously inspected for leaks and purged with nitrogen to eliminate atmospheric oxygen. Subsequently, the pressure was adjusted to approximately 0.5 MPa, and the furnace was turned on. After reaching the target temperature, the furnace was switched off, and the system was allowed to cool to ambient conditions. The gases generated during the process were collected using a gasometer. Once cooled, the reactor lid was replaced with a specialized distillation head. The accumulated liquid products were then distilled under atmospheric pressure (1 atm) across the following temperature ranges: >180 °C, 180–240 °C, and 240–320 °C. The resulting fractions were condensed in a cooling unit and collected by gravity into a receiving flask. The solid residue remaining in the reactor was manually removed after each experiment. To ensure the reliability and reproducibility of the results, each experiment was repeated three times under identical conditions. The variation in results did not exceed 2%. Based on the experimental data, a schematic diagram illustrating the coking process of heavy oil residues using residual engine oils is presented in Fig. 1.

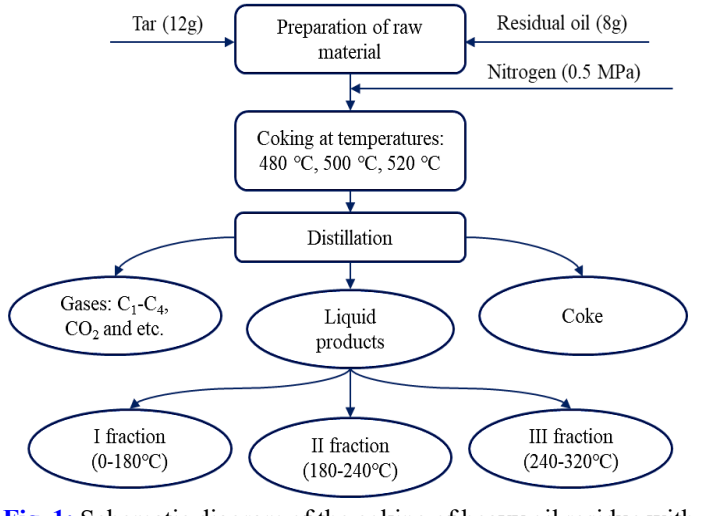

Fig. 1: Schematic diagram of the coking of heavy oil residue with residual engine oils.

2.2 Chromatographic analysis

Determination of the fractional composition of the resulting gasoline fraction was carried out using a Chromatec-Krystal 5000 apparatus to determine the composition of the analyzed oil fractions according to the standards ISO 3405. While samples of light and heavy gas oil fractions were analyzed on an Agilent 7890A/5975C GC-MS gas chromatography-mass spectrometer (USA). Conditions for chromatographic analysis: mobile phase - helium; evaporator temperature 290 °C, flow recovery (separation) 500:1; column temperature: at the beginning 40 °C, temperature increase 4 °C per minute, at the end 310 °C, holding at the final temperature for 2 minutes,

total analysis time 80 minutes; The ionization of the mass detector was carried out by the electron impact method. The type of capillary column of the apparatus is HP-5 MS, column length is 30 m, internal diameter is 0.25 mm, and the stationary phase is dimethylpolysiloxane.

2.3 Raman spectroscopy

Chemical bonds and compounds have a significant influence on the structure of coke. Cokes with different structures can be well identified using the vibrational movements of their skeleton in Raman spectra.[20,21] Experiments were performed on a LabRam HR800 Raman spectrometer (HORIBA Jobin Yvon Raman Division, France) exposed to a 473 nm blue laser with 35 mW power (ND=0.5 and ND=1 filters) and a 600/600 grating. The peaks around 1590 cm^{-1} and 1350 cm^{-1} are characteristic of defects in graphitic structures.

2.4 Scanning electron microscopy (SEM)

SEM is a widely used method for analyzing the surface characteristics of coke.[22] The microstructure and morphology of coke obtained after the experiments were determined using a low-vacuum SEM JSM 6610LV (Joel, USA). Effective diameter of the electron probe in secondary electrons at 30 kV: <30 nm. Magnification adjustment range: 8/300000x. Measuring range of linear dimensions: 0.15/5000 µm. Limits of permissible relative error in measurements of linear dimensions: in the range from 0.15 to 0.3 µm ± 11%; in the range from 0.3 to 0.6 µm ± 7%; in the range from 0.6 to 5000 µm ± 5%.

2.5 Optical microscopy

The formation of coke was analyzed using a Leica DM600 M automated digital optical microscope.

2.6 Brunauer-Emmett-Teller (BET) analysis

The porous structure of the resulting coke samples was studied using an ASAP 2400 analyzer (Micromeritics Instrument, USA). Prior to measurements, the samples were degassed under vacuum at 200 °C for 12 hours to ensure complete removal of adsorbed impurities, with the residual pressure not exceeding 0.001 mmHg.

2.7 Infrared spectroscopy (IR) analysis

IR spectra were recorded using a Vertex 70 FTIR spectrometer (Bruker) equipped with a software-controlled system. The measurement parameters were as follows: resolution of 4 cm^{-1}, 16 scans for both background and sample (relative to air), and a spectral range of 500–4000 cm^{-1}.

2.8 Determination of total moisture content of coke

Moisture content of coke was performed according to the ISO 1171:2024 "Coal and coke — Determination of ash". The tray was weighed with an accuracy of 0.1 g (m_1). Approximately 100 g ± 1 g of the coke sample was distributed over the tray and reweighed with the same accuracy (m_2). The tray with coke was placed in an oven and treated at a temperature of 120 °C to 200 °C. The tray with the dried sample was removed and immediately reweighed with an accuracy of 0.1 g (m_3) to prevent moisture absorption. The mass fraction of total moisture (M_T) is determined by the following Eq. (1):

$$M_T = \frac{m_2 - m_3}{m_2 - m_1} \times 100 \quad (1)$$

where m_1 is the mass of the empty tray (g), m_2 is the mass of the tray plus coke before heating (g), and m_3 is the mass of the tray plus coke after heating (g).

2.9 Determination of volatile matter content in coke

Volatile matter content in coke was performed according to the ISO 562-2024 "Hard coal and coke — determination of volatile matter content". The initial stage was the preheating of the crucibles at 900°C ± 5°C for 7 minutes. The weight of crucibles, cooled to room temperature, was measured to the nearest 0.1 mg (m_1). Then, a 1 g ± 0.1 g sample of petcoke was weighed into the crucibles (m_2). Three drops of cyclohexane were added to prevent oxidation. The crucibles with samples were transferred to the furnace and heated at 900 °C ± 5 °C for 7 minutes ± 5 seconds. After cooling, the final weight of each crucible was recorded on the same precision balance (m_3). The mass fraction of volatile substances (V) is determined by the following Eq. (2):

$$V = \frac{(m_2 - m_3) \times 100}{m_2 - m_1} - \omega_{H_2O} \quad (2)$$

where m_1 is the mass of the crucible and lid (g), m_2 is the mass of the crucible and lid and coke sample before the heating (g), m_3 is the mass of the crucible and lid and contents after heating (g), and ω_{H_2O} is the moisture in the sample as analyzed (%).

2.10 Determination of ash content of coke

Ash content of coke was performed according to the ISO 1171:2024 "Coal and coke — Determination of ash". The dish was weighed to the nearest 0.1 mg (m_1). About 1 g of the sample was evenly spread in the dish and was reweighed (m_2). The dish was placed in the furnace at a temperature of 815 °C ± 10 °C, where it remained for 60 minutes. The dish was removed and cooled on a thick metal plate for 10 minutes, then transferred to a desiccator and cooled to room temperature before weighing to the nearest 0.1 mg (m_3). The ash content (A) is determined by the following Eq. (3):

$$A = \frac{m_3 - m_1}{m_2 - m_1} \times 100 \quad (3)$$

where m_1 is the mass of empty dish (g), m_2 is the mass of dish plus test portion (g), and m_3 is the mass of dish plus ash (g).

3. Results and discussion

3.1 Chromatographic analysis of distillates at different temperatures

The results of chromatographic analysis of fractions of gasoline, light gas oil, and heavy gas oil by atmospheric distillation obtained by coking petroleum residues in the presence of residual engine oil are demonstrated in Tables 1-3. The results have shown a varied distribution of different types of hydrocarbons across the gasoline fraction, light gas oil fraction, and heavy gas oil fraction.

At 480 °C (Table 1), the gasoline fraction exhibited a notably higher proportion of alkanes (33.54%), whereas aromatic hydrocarbons were more concentrated in the heavy gas oil fraction (10.18%). In contrast, during the coking process at 500 °C, the gasoline fraction contained the highest percentage of aromatic hydrocarbons (25.83%), while the heavy gas oil fraction showed a substantial proportion of alkanes (19.14%). At 520 °C, the alkane concentration increased progressively from the gasoline fraction (17.09%) to the heavy gas oil fraction (24.30%). The elevated percentage of alkanes in the heavy gas oil fraction at this temperature may be attributed to the higher boiling points of alkanes compared to other hydrocarbon classes.

Moreover, the coking temperature significantly influenced the distribution of other hydrocarbon groups across the different fractions.[23] At 480 °C, the gasoline fraction contained a relatively high concentration of isoalkanes (31.79%). In contrast, at 520 °C, the highest percentage of isoalkanes (20.94%) was observed in the light gas oil fraction. The distribution of alkenes and cycloalkanes also varied with temperature, with the maximum concentration of cycloalkanes (17.30%) detected in the gasoline fraction at 480 °C.

The high percentage of aromatic hydrocarbons in the gasoline fraction at 500 °C (Table 2) can be attributed to the elevated coking temperature, which promotes the formation of aromatic structures.[24,25] The coking of heavy oil waste at 500 °C and 520 °C demonstrated that temperature had a significant effect on the chemical composition of the distillates. At 500 °C, aromatic hydrocarbons were the predominant component across all fractions, with the highest concentration observed in the gasoline fraction (25.83%). At 520 °C (Table 3), the concentration of aromatic hydrocarbons increased in all fractions, reaching 38.52% in the gasoline fraction. These results indicate that higher temperatures favor the formation of aromatic compounds, likely due to the enhanced thermal breakdown of complex hydrocarbons into simpler aromatic structures at elevated temperatures.[26]

The tables demonstrate that aromatic hydrocarbons and alkanes are the predominant components in the liquid fractions. The elevated aromatic content is likely attributable to the

Table 1: Chemical composition of distillates obtained at 480 °C

Group chemical composition of hydrocarbons	Gasoline fraction, 0-180 °C	Light gas oil fraction, 180-240 °C	Heavy gas oil fraction, 240-320 °C
Alkanes	33.54	28.21	21.60
Isoalkanes	31.79	13.21	8.33
Alkenes	10.12	7.04	4.53
Cycloalkanes	17.30	2.80	0.37
Aromatic hydrocarbons	6.68	8.13	10.18

Table 2: Chemical composition of distillates obtained at 500 °C.

Group chemical composition of hydrocarbons	Gasoline fraction, 0-180 °C	Light gas oil fraction, 180-240 °C	Heavy gas oil fraction, 240-320 °C
Alkanes	15.53	17.82	19.14
Isoalkanes	3.57	1.36	0.98
Alkenes	7.44	2.56	4.53
Cycloalkanes	2.19	2.25	1.24
Aromatic hydrocarbons	25.83	9.84	11.35

Table 3: Chemical composition of distillates obtained at 520 °C.

Group chemical composition of hydrocarbons	Gasoline fraction, 0-180 °C	Light gas oil fraction, 180-240 °C	Heavy gas oil fraction, 240-320 °C
Alkanes	17.09	13.76	24.30
Isoalkanes	6.58	20.94	9.76
Alkenes	7.46	14.57	10.85
Cycloalkanes	12.43	9.85	7.64
Aromatic hydrocarbons	38.52	20.68	23.19

inherent presence of aromatic compounds in the heavy oil residue. Moreover, the results indicate that the coking temperature exerts a significant influence on the chemical composition of the resulting distillates. A comprehensive understanding of the mechanisms driving these compositional changes may enable the optimization of the coking process to selectively produce hydrocarbon fractions with desired characteristics.

3.2 IR spectroscopy of coke

The IR spectra of all samples are presented in Fig. 2, with the corresponding functional groups identified for each peak listed in Table 4.[27] Variations in the positions and intensities of the absorption bands were observed across the spectra, indicating changes in the chemical composition of the coke samples as a function of coking temperature.

Table 4: IR spectroscopy peak identification.[27]

Peak	Wavenumber (cm^{-1})	Vibration/Functional group
A	3442	υ (–OH)
B	2927	δ ($–CH_3$) aliphatic
C	2366	υ (COOH) residual oxygen bands
D	1632	υ (–H) aromatic hydrogen
E	1438	υ ($–CH_2–$, $–CH_3$)
F	1383	δ($–CH_3$)
G	1127 1004	υ (Si–O) ash
H	873 753	υ (CH) aromatic

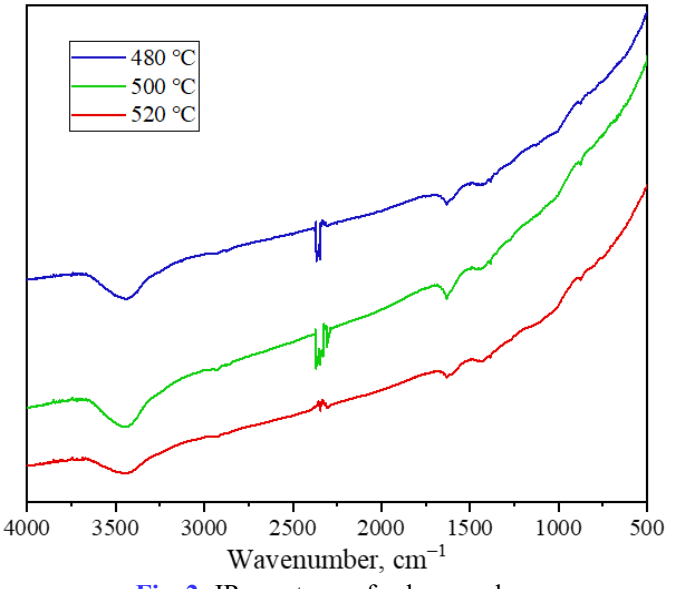

Fig. 2: IR spectrum of coke samples.

The obtained IR spectra exhibit complex peak profiles, from which key structural features can be identified. Characteristic C–H out-of-plane bending vibrations of aromatic compounds are observed at 873 cm^{-1} and 750 cm^{-1}, while the stretching vibration associated with aromatic C=C bonds appears at 1632 cm^{-1}, indicating the presence of condensed aromatic structures in the coke. The increased intensity of these bands in the second and third coke samples suggests enhanced aromatization and graphitization at higher coking temperatures, likely due to thermal effects similar to calcination. Peaks labeled B, E, and F are indicative of alkyl fragments, and the absorption band near 2927 cm^{-1} corresponds to residual aliphatic C–H bonds. Notably, the intensity of these aliphatic bands decreases with increasing temperature, reflecting the progressive degradation of aliphatic chains and a concomitant increase in the aromatic character of the coke. The peak at 2366 cm^{-1}, attributed to the asymmetric stretching of –COOH groups, suggests the presence of residual oxygen-containing compounds derived from tar in the first two samples. In the third sample, a marked reduction in the intensity of this peak implies the removal of oxygen-containing functional groups at elevated temperatures, consistent with calcination-like behavior. The broad absorption band around 3442 cm^{-1} is associated with O–H stretching vibrations, which may originate from hydroxyl functional groups or adsorbed moisture. A decrease in the intensity of this band with rising temperature indicates thermal dehydration. Additionally, bands at 1127 cm^{-1} and 1004 cm^{-1} correspond to mineral residues (ash content), and their relatively constant intensity across the samples suggests that the inorganic content remains stable over the investigated temperature range.

As the coking temperature increases, significant structural transformations occur in the coke. Specifically, the content of aliphatic fragments and oxygen-containing functional groups decreases, while the proportion of aromatized carbon structures increases. These changes enhance the graphite-like characteristics of the material. Therefore, the optimal coking temperature should strike a balance between maximizing aromaticity and minimizing material losses due to the release of gaseous by-products.

3.3 Raman spectroscopy of coke samples

The spectra of three coke samples obtained at 480, 500, and 520 °C and the curve-fitting Raman spectrum of coke obtained at 500 °C are illustrated in Figs. 3a and 3b, respectively. Meanwhile, band information from curve-fitting is given in Table 5. The Raman shift, which corresponds to the vibrational modes of the carbon atom bonds, identified peaks between 1000 cm^{-1} and 1700 cm^{-1}. These peaks are characteristic of graphitic and amorphous carbon structures, and their intensity is directly proportional to the number of molecules contributing to that vibrational mode.[28,29]

Previous Raman spectroscopy studies on carbon structure characteristics of cokes indicate that crucial information can be obtained from two peaks located at regions between 1350 and 1380 cm^{-1} (D band) and also 1580 and 1600 cm^{-1} (G band).[30-32] D-band indicates the disordered or defective sp^2-bonded carbon, or impurities in the graphitic structure of coke,

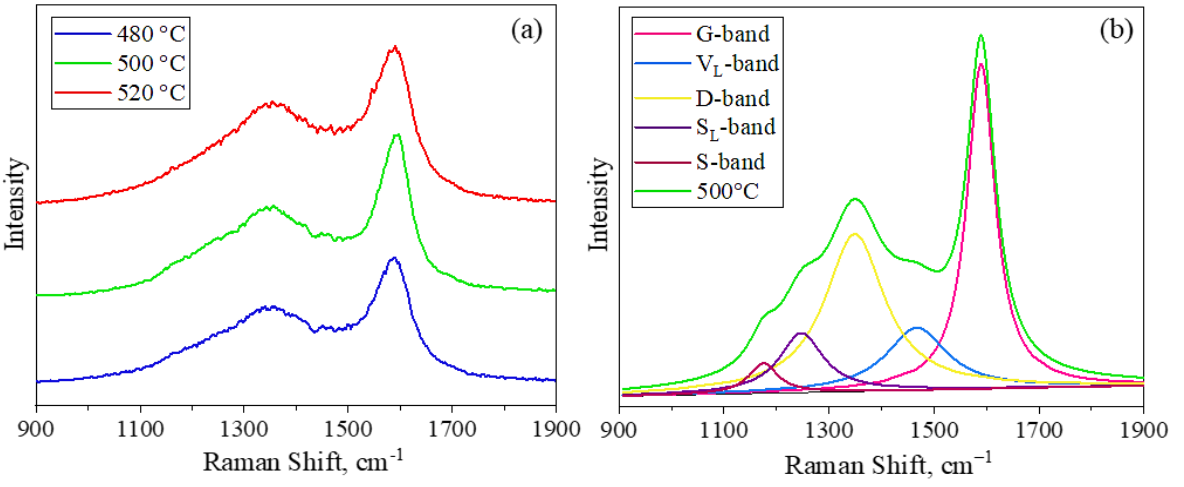

Fig. 3: (a) Raman spectra of coke samples and (b) curve-fitting Raman spectrum of coke obtained at 500 °C.

while G-band corresponds to the stretching of sp²-bonded carbon atoms in a graphitic lattice and domains. The intensity and sharpness of these two bands vary among the samples and reflect that structural disorder differs depending on process temperature. The mild oxidation causes disorder by forming defects from the breakage of sp^2 hybridization and the formation of functional groups. These groups are detected in the IR study as well (Table 5).[33]

The results of the calculation of the structural parameters are presented in Table 6. The I_D/I_G ratio, the relative intensity of the D-band compared to the G-band, indicates the relative amount of defects in the graphite domains and provides information on the quality of the structure.[34]

It can be seen that the values of G–D and I_D/I_G increase and decrease, respectively, when the cooking temperature increases. The G–D band difference increases from 228 cm^{-1} to 243 cm^{-1}, indicating a decrease in amorphous carbon and an increase in the size of aromatic clusters.[27,35] The I_D/I_G ratio decreases from 0.627 (480 °C) to 0.485 (520 °C). Lower I_D/I_G ratios indicate a higher degree of graphitization, which means that the coke produced at 520 °C has a more ordered and stable carbon structure. This trend is consistent with the expectation that higher coking temperatures promote dehydrogenation and polycondensation of aromatic rings, resulting in a more graphitized structure.

Altogether, as temperature increases, functional groups with heteroatoms are destroyed as a result, defects and disorder of crystallites in aromatic structures seem to decrease, which correlates with an increase in the degree of coke graphitization. These results indicate that coking temperature plays an important role in optimizing the coke structure while balancing the disorganization required for reactivity and the graphitization required for mechanical strength.

Table 5: Literature data of Raman spectroscopy.[33]

Band name	Sample			Characteristics
	1	2	3	
S	–	1175	–	C_{ar}–C_{al}; aromatic ethers; C–C on hydroaromatic rings; C–H on aromatic rings
S_L	1245	1246	1234	Aryl-alkyl ether; para-aromatics
D	1358	1351	1354	C bands of highly ordered carbon materials, C–C between aromatic rings and aromatics with not less than 6 rings
V_L	1493	1468	1471	$–CH_3$; $–CH_2–$; Breathing vibration of semi-aromatic ring, Amorphous carbon structures
G_R	–	–	1561	Aromatics with 3-5 rings; Amorphous carbon structures
G	1586	1591	1597	Aromatic ring breathing; Alkene C=C

Table 6: Results of calculation from Raman data.

Sample	Coking temperature, °C	D, cm^{-1}	G, cm^{-1}	G–D, cm^{-1}	I_D/I_G
1	480	1358	1586	228	0.627
2	500	1351	1591	240	0.578
3	520	1354	1597	243	0.485

3.4 The microstructure and morphology of coke

The SEM was used to investigate the microstructure and morphology of coke derived from a recirculating agent under different conditions. The surface morphology of the obtained coke was examined using optical microscopy at magnifications of 1000× and 2000× (Fig. 4), as well as SEM at a magnification of 5000× for detailed structural analysis (Fig. 5).

Optical microscopy of the sample obtained at 480 °C (Fig. 4a) reveals relatively large pores and irregular structural features, indicative of incomplete carbonization. The presence of unreacted material and gas bubbles suggests a low degree of structural ordering. In contrast, the sample produced at 500 °C (Fig. 4b) exhibits a more compact and crystalline coke structure with enhanced graphitization. The observed reduction in porosity suggests a transition towards a denser and more ordered material. Further structural development is evident in the sample obtained at 520 °C (Fig. 4c), which displays a well-defined anisotropic texture, indicative of a higher degree of carbonization and the emergence of graphite-like domains. Overall, with increasing temperature, the coke structure becomes progressively denser, exhibiting more distinct crystalline regions and reduced porosity characteristics that may limit its suitability for applications such as electrode production.

Coke conglomerates with varying lengths and diameters were identified across the samples. The diameter of the coke particles ranged from 643 nm to 1.81 μm, while the lengths varied from 409.0 nm to 3.20 μm. Additionally, some coke particles were observed to be encapsulated within carbonlayers. SEM micrographs of the coke surface from the 480 °C sample revealed a dense and finely dispersed amorphous morphology, further supporting the conclusion of limited structural ordering at lower coking temperatures.

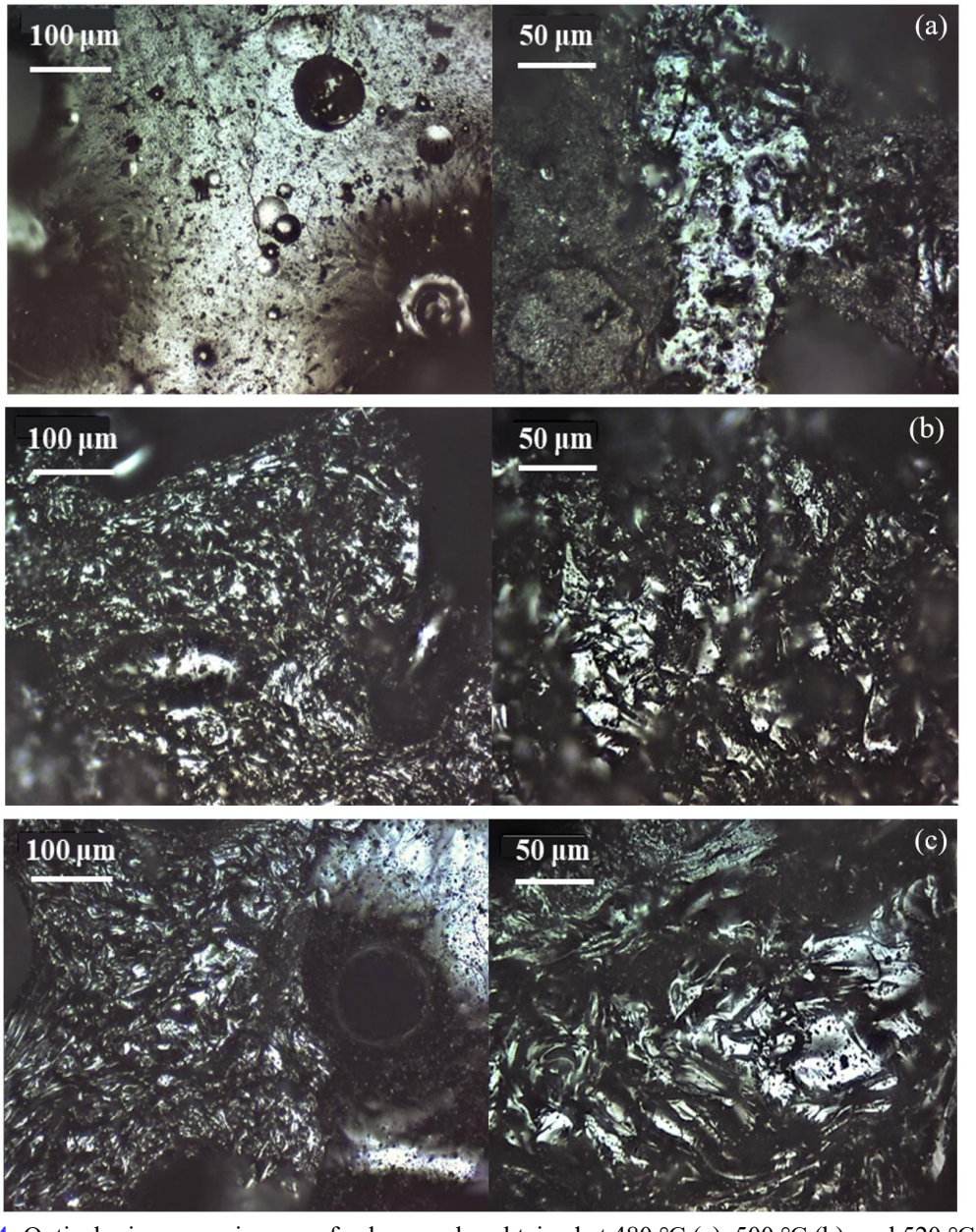

Fig. 4: Optical microscope images of coke samples obtained at 480 °C (a), 500 °C (b), and 520 °C (c).

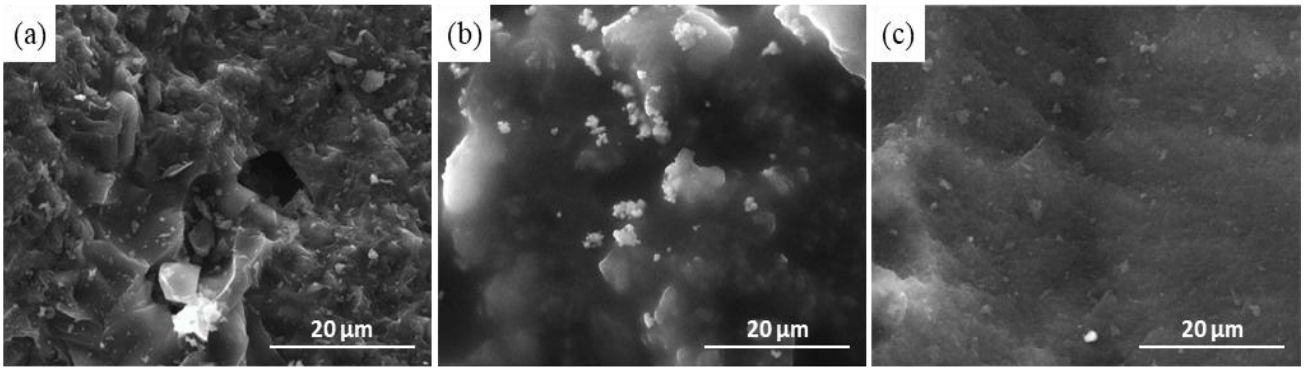

Fig. 5: SEM micrographs of coke obtained at (a) 480 °C, (b) 500 °C, and (c) 520 °C.

A comparison of the microstructural images of coke samples obtained at 500 °C (Fig. 5b) and 520 °C (Fig. 5c), under identical conditions (0.5 MPa pressure and 4-hour processing time), reveals notable morphological differences. At 500 °C, the coke particles exhibit more sharply defined contours and the formation of hollow structures, suggesting a more organized microstructure. In contrast, the micrographs of the sample produced at 520 °C display numerous scattered white particles that are irregular in both shape and size, indicative of structural heterogeneity and potential surface degradation.[36] These observations suggest that the coke formed at 500 °C possesses a more developed and coherent structure compared to that produced at the higher temperature, where excessive thermal energy may lead to microstructural disruption and reduced uniformity. Coke is characterized by a detailed, fine-grained structure. The size of the rough granular mosaic and its moderately rough look are evident. Observations also include the depth of the pores and the fine granular structure near the pore wall.[37,38] The image reveals irregular and shapeless structures, akin to the associated shot type, coke.

3.5 Surface porosity of coke

Some chemical and physico-chemical properties of coke, which determine its quality, are defined by the surface structure of coke and its porosity. For example, the reactivity of coke largely depends on the size of its internal specific surface. In the total specific surface area of coke, the main place is occupied by the internal specific surface. Therefore, the methods for determining the specific surface area of coke offer sufficiently accurate information about the value of its internal specific surface. The specific surface of micropores varies in different cokes with different degrees of burnup from 16 to 600 m^2/g.[39-41] The results of the specific surface area study of the obtained coke, conducted using the BET method, are presented in Table 7, which displays the results of two separate experiments.

At 500 °C, the specific surface area was found to be 67.6 m^2/g. However, when the temperature was increased to 520 °C, the specific surface area decreased significantly to 13.1 m^2/g. The specific surface area of coke, which is a measure of the available reactive surface of the coke, was found to decrease with an increase in temperature from 500 °C to 520 °C. This could be linked to the fact that elevated temperatures lead to a higher degree of graphitization, reducing the number of active sites available on the coke surface. The significant decrease in the specific surface area with a relatively small increase in temperature suggests that the coking is a temperature-dependent process.[42,43] This is essential for the regulation of the coking process and for the production of coke. However, it is important to underline that those other factors, such as the composition of the tar and the presence of a recirculating agent, could also influence the specific surface area of the coke. Further investigations are required to have a better understanding of the interconnections and to enhance the efficiency of the coking process.

3.6 Coke quality

The quality and type of obtained coke is determined by analysis of ash content, total moisture and volatile substances, the results of which are given in Table 8. Comparison with literature data provides insight into its implications for industrial applications.[44]

Ash contents at 480 °C (1.08 %), 500 °C (0.34 %), and 520 °C (0.55 %) were found to be almost within the range reported in the electrode literature (0.1-1.0%) but higher than

Table 7: Specific surface areas of cokes obtained at 480, 500, and 520 °C.

Experiments	1	2	3	Average
Specific surface area, m^2/g; 480 °C	90.6	95.4	96.5	94.2
Specific surface area, m^2/g; 500 °C	67.2	68.1	67.5	67.6
Specific surface area, m^2/g; 520 °C	13.0	13.4	12.9	13.1

Table 8: Technical parameters (indicators) of petroleum coke.

Quality characteristics	Sample			Literature data[44]	
	1	2	3	Electrode	Coke fines
Ash content, %	1.08	0.34	0.55	0.1 – 1.0	0.8
Mass fraction of total moisture, %	4.54	4.46	3.09	3.0	3.0
Mass fr. of volatile substances, %	6 .61	7.22	6.20	7.0 – 9.0	11.5

coke fines (0.8%). The increase in ash content with temperature suggests that the combustion process may be more complete at higher temperatures, resulting in higher concentrations of inorganic contaminants and non-combustible residues.[45] High ash content may result in slag formation, which may cause disposal problems. In addition, ash content should be maintained below 0.3% for anode production.

The total moisture content was higher in the experiments (4.54% at 480 °C, 4.46% at 500 °C, and 3.09% at 520 °C) compared to the literature data (3.0% for both electrodes and coke breeze). The higher moisture content in the experimental results may be due to the hygroscopicity.[28] of the obtained coke samples. If the sample has a high affinity for water, it can absorb moisture from the environment, resulting in high moisture content.

The volatile matter content decreased with temperature from 6.61% at 480 °C to 7.22% at 500 °C and 6.20% at 520 °C. The values at 480 °C and 500 °C are in the range of literature data for electrodes (7.0 - 9.0%), while the value at 520 °C is close to the value for coke fines (11.5%). The decrease in the mass fraction of volatiles with temperature can be explained by the thermal decomposition of the material.[29] With increasing temperature, more volatile compounds can be released. This can have important implications for the use of these materials in industrial processes, since the release of volatiles can affect the efficiency and safety of the process. The results of this study indicate that the coke obtained in this study can be recommended for industrial use.

3.7 Sulfur content

The sulfur content of coke and liquid products when coking heavy oil waste in the presence of a recycling agent is indicated in Table 9.

The sulfur content varies significantly among the different products, with the highest content found in coke (0.930%) and the lowest in gasoline (0.132%). This suggests that the coking process may concentrate sulfur in the solid coke product, while the lighter fractions (gasoline and gas oils) contain less sulfur.

The gasoline fraction exhibited the lowest sulfur content, measuring 0.132% at 500 °C and increasing slightly to 0.185% at 520 °C. Light gas oil showed a sulfur content of 0.802% at 500 °C, which rose to 0.967% at 520 °C. Similarly, the sulfur content in heavy gas oil increased from 0.432% to 0.759% over the same temperature range. These trends indicate that all liquid fractions tend to accumulate more sulfur as the temperature increases. Notably, the sulfur content in coke showed a significant rise, from 0.930% at 500 °C to 1.146% at 520 °C. This suggests that sulfur compounds in the feedstock are increasingly retained in the solid residue at higher temperatures.

The sulfur content of the resulting coke can be reduced through thermal dehydration. Increasing both the temperature and pressure during this step has been shown to lower sulfur content by up to 2.5%, thereby improving coke quality.[46,47] Although the addition of a recycling agent enhanced coke yield from heavy oil waste, the coke still retained a considerable amount of sulfur after the coking process. In light gasoline, the content of sulfur increases significantly compared to gasoline. This could be due to the fact that light gas oil is a heavier fraction compared to gasoline, and thus contains more sulfur compounds. Interestingly, the sulfur content decreased slightly in heavy gas oil.[48] The results indicate that liquid fractions derived from coking processes have a relatively low sulfur content, which is desirable for standard requirements and environmental reasons. This indicates that the approach applied in this study shows good potential for sulfur mitigation.

3.8 Material balance

The material balance analysis demonstrates that the majority of the input feedstock is converted into distillates, highlighting the efficiency of the process in producing liquid products (Table 10). The relatively low yield of coke and gaseous products, along with minimal mass loss, indicates favorable operational conditions. These results are essential for evaluating the effectiveness of the cooking process and serve as a basis for further optimization of feed composition and process parameters.

The process utilized two input materials: 12 g of petroleum residues and 8 g of residual engine oil, resulting in a total feed mass of 20 g. Upon completion of the coking process, four distinct output streams were identified. The solid coke product accounted for 3.73 g, while distillates represented the major fraction at 14.62 g, corresponding to 73.1% of the total output. Gaseous products constituted a smaller portion, amounting to 1.34 g. A minor discrepancy of 0.31 g, or 1.55%

Table 9: The content of sulfur in products formed during coking, mass. %.

Sample number	Coking temperatures	Components			
		Gasoline	Light gas oil	Heavy gas oil	Coke
1	480 °C	0.095	0.672	0.235	0.780
2	500 °C	0.132	0.802	0.432	0.930
3	520 °C	0.185	0.967	0.759	1.146

Table 10: Material balance of the process.

Input	m, g	% by mass	Output	m, g	% by mass
Petroleum residues (tar) and residual engine oils	12	60	Coke	3.73	18.65
			Distillates	14.62	73.1
	8	40	Gas	1.34	6.7
			Loss	0.31	1.55
Overall	20	100	Overall	20	100

of the total input mass, was recorded as process loss. This material balance offers valuable insight into the distribution of products and the overall efficiency of the thermal conversion process. This material balance offers an overview of the process flow and the distribution of various components across different stages. It serves as a valuable tool for assessing process efficiency and identifying opportunities for optimization.

4. Conclusion

The findings of this study demonstrated that 18.65% of the total output was coke, while distillates constituted the majority at 73.1%, indicating a high potential for fuel recovery. The hydrocarbon group composition of the liquid fractions closely resembles that of primary atmospheric distillation fractions of crude oil, suggesting that the process is effective for the refinement of heavy petroleum residues. The produced coke exhibited relatively low ash content - 0.34% at 500 °C and 0.55% at 520 °C - along with sulfur contents of 0.930% and 1.146%, respectively. The low ash content implies minimal residual matter following combustion, facilitating easier disposal and enhancing the suitability of the coke for electrode applications. Sulfur content is also a critical factor, as elevated sulfur levels contribute to sulfur dioxide emissions during combustion, a major environmental concern.

IR spectroscopy confirmed an increase in coke aromaticity with rising temperature, while Raman spectroscopy revealed enhanced graphitization, consistent with observations from SEM and optical microscopy. The gradual reduction of disordered carbon structures and the corresponding growth in graphitic domain size further support the formation of structurally advanced coke at higher temperatures. These results collectively indicate that the produced coke possesses favorable structural and compositional characteristics for industrial use. Based on experimental results, the optimal conditions for the coking process were identified as a temperature of 500 °C, a recycling coefficient of 1.5, and a pressure of 0.5 MPa. These parameters are crucial for potential scale-up and industrial implementation of the process.

Acknowledgements

This study was supported by the Science Committee of the Ministry of Science and Higher Education of the Republic of Kazakhstan (AP19679889)

Conflict of Interest

There is no conflict of interest.

Supporting Information

Not applicable.

References

[1] A. Guo, Y. Zhou, K. Chen, Z. Xue, Z. Wang, H. Song, Co-processing of vacuum residue/fraction oil blends: Effect of fraction oils recycle on the stability of coking feedstock, *Journal of Analytical and Applied Pyrolysis*, 2014, **109**, 109-115, doi: 10.1016/j.jaap.2014.07.006.

[2] A. N. Sawarkar, A. B. Pandit, S. D. Samant, J. B. Joshi, Petroleum residue upgrading via delayed coking: A review. *The Canadian Journal of Chemical Engineering*, 2007, **85**, 1-24, doi: 10.1002/cjce.5450850101.

[3] X. Dong, H. Liu, Z. Chen, K. Wu, N. Lu, Q. Zhang, Enhanced oil recovery techniques for heavy oil and oilsands reservoirs after steam injection, *Applied Energy*, 2019, **239**, 1190-1211, doi: 10.1016/j.apenergy.2019.01.244.

[4] J. Taheri-Shakib, A. Shekarifard, H. Naderi, Heavy crude oil upgrading using nanoparticles by applying electromagnetic technique, *Fuel*, 2018, **232**, 704-711, doi: 10.1016/j.fuel.2018.06.023.

[5] P. Solanki, D. Baldaniya, D. Jogani, B. Chaudhary, M. Shah, A. Kshirsagar, Artificial intelligence: New age of transformation in petroleum upstream, *Petroleum Research*, 2022, **7**, 106-114, doi: 10.1016/j.ptlrs.2021.07.002.

[6] I. J. Okeke, T. A. Adams, Combining petroleum coke and natural gas for efficient liquid fuels production, *Energy*, 2018, **163**, 426-442, doi: 10.1016/j.energy.2018.08.058.
[7] V. M. Kapustin, V. F. Glagoleva, Physicochemical aspects of petroleum coke formation, *Petroleum Chemistry*, 2016, **56**, 1-9, doi: 10.1134/S0965544116010035.
[8] J. Li, Q. Xiong, J. Shan, J. Zhao, Y. Fang, Investigating a high vanadium petroleum coke ash fusibility and its modification, *Fuel*, 2018, **211**, 767-774, doi: 10.1016/j.fuel.2017.09.110.
[9] S. Kumar, M. Srivastava, Influence of presence/addition of asphaltenes on semi-coke textures and mesophase development in petroleum feed stocks, *Fuel*, 2016, **173**, 69-78, doi: 10.1016/j.fuel.2016.01.026.
[10] M. A. Flórez, J. E. Guerrero, R. Cabanzo, E. Mejía-Ospino, SARA analysis and Conradson carbon residue prediction of Colombian crude oils using PLSR and Raman spectroscopy, *Journal of Petroleum Science and Engineering*, 2017, **156**, 966-970, doi: 10.1016/j.petrol.2017.06.007.
[11] Z. Xiong, S. S. A. Syed-Hassan, X. Hu, J. Guo, J. Qiu, X. Zhao, S. Su, S. Hu, Y. Wang, J. Xiang, Pyrolysis of the aromatic-poor and aromatic-rich fractions of bio-oil: Characterization of coke structure and elucidation of coke formation mechanism, *Applied Energy*, 2019, **239**, 981-990, doi: 10.1016/j.apenergy.2019.01.253.
[12] L. Tian, B. Shen, J. Liu, A delayed coking model built using the structure-oriented lumping method, *Energy & Fuels*, 2012, **26**, 1715-1724, doi: 10.1021/ef201570s.
[13] E. M. A. Edreis, X. Li, C. Xu, H. Yao, Kinetic study and synergistic interactions on catalytic CO_2 gasification of Sudanese lower sulphur petroleum coke and sugar cane bagasse, *Journal of Materials Research and Technology*, 2017, **6**, 147-157, doi: 10.1016/j.jmrt.2016.09.001.
[14] V. N. Rubchevskiy, S. A. Ovchinnikova, V. M. Volokh, R. A. Begma, L. P. Bannikov, V. V. Karchakova, Influence of coking parameters on the quality of tar for electrode-pitch production, *Coke and Chemistry*, 2014, **57**, 158-162, doi: 10.3103/S1068364X14040061.
[15] Y. Liu, M. Sun, Q. Yao, L. He, T. Yan, G. Fei, Advancements, mechanisms, and challenges in the catalytic conversion of coal, coal tar, model compounds, and coal+ x: An in-depth analysis of light aromatics preparation and future perspectives, *Fuel*, 2025, **385**, 134094, doi: 10.1016/j.fuel.2024.134094.
[16] C. Liu, Z. Xie, F. Sun, L. Chen, Exergy analysis and optimization of coking process, *Energy*, 2017, **139**, 694-705, doi: 10.1016/j.energy.2017.08.006.
[17] M. Liu, F. Chu, J. He, D. Yang, C. Chu, Coke production scheduling problem: A parallel machine scheduling with batch preprocessings and location-dependent processing times, *Computers & Operations Research*, 2019, **104**, 37-48, doi: 10.1016/j.cor.2018.12.002.
[18] K. Toshtay, A. B. Auyezov, Z. A. Bizhanov, A. T. Yeraliyeva, S. K. Toktasinov, B. Kudaibergen, A. Nurakyshev, Effect of catalyst preparation on the selective hydrogenation of vegetable oil over low percentage Pd/diatomite catalysts, *Eurasian Chemico-Technological Journal*, 2015, **17**, 33-39, doi: 10.18321/ectj192.
[19] Y. Cheng, L. Yang, C. Fang, X. Guo, Co-carbonization behavior of petroleum pitch/graphene oxide: Influence on structure and mechanical property of resultant cokes, *Journal of Analytical and Applied Pyrolysis*, 2016, **122**, 387-394, doi: 10.1016/j.jaap.2016.08.019.
[20] M. A. den Hollander, M. Makkee, J. A. Moulijn, Coke formation in fluid catalytic cracking, catalyst deactivation, *Proceedings of the 7th International Symposium*, 1997, 295-302, doi: 10.1016/s0167-2991(97)80167-x.
[21] C. C. Zhang, S. Hartlaub, I. Petrovic, B. Yilmaz, Raman spectroscopy characterization of amorphous coke generated in industrial processes, *ACS Omega*, 2022, **7**, 2565-2570, doi: 10.1021/acsomega.1c03456.
[22] A. Ali, N. Zhang, R. M. Santos, Mineral characterization using scanning electron microscopy (SEM): A review of the fundamentals, advancements, and research directions, *Applied Sciences*, 2023, **13**, 12600, doi: 10.3390/app132312600.
[23] B. Shi, S. K. Ngueleu, F. Rezanezhad, S. Slowinski, G. J. Pronk, C. M. Smeaton, K. Stevenson, R. I. Al-Raoush, P. Van Cappellen, Sorption and desorption of the model aromatic hydrocarbons naphthalene and benzene: effects of temperature and soil composition, *Frontiers in Environmental Chemistry*, 2020, **1**, 581103, doi: 10.3389/fenvc.2020.581103.
[24] H. Yu, T. Hu, Y. Mao, T. Liao, M. Shi, W. Liu, M. Li, Y. Yu, Y. Zhang, X. Xing, S. Qi, Influence of temperature and precipitation on the fate of polycyclic aromatic hydrocarbons: simulation experiments on peat cores from a typical alpine peatland in Central China, *Environmental Science and Pollution Research*, 2023, **30**, 37859-37874, doi: 10.1007/s11356-022-24559-4.
[25] Y. Qian, Y. Qiu, Y. Zhang, X. Lu, Effects of different aromatics blended with diesel on combustion and emission characteristics with a common rail diesel engine, *Applied Thermal Engineering*, 2017, **125**, 1530-1538, doi: 10.1016/j.applthermaleng.2017.07.145.
[26] N. S. Mussa, K. Toshtay, M. Capron, Catalytic applications in the production of hydrotreated vegetable oil (HVO) as a renewable fuel: a review, *Catalysts*, 2024, **14**, 452, doi: 10.3390/catal14070452.
[27] S. Yang, Q. Pang, T. Xu, Z. He, T. Song, J. Zhang, FTIR and Raman spectroscopy characterization of coking coals with diverse coalification, *Coke and Chemistry*, 2019, **62**, 211-219, doi: 10.3103/s1068364x19060085.
[28] M. Fredriksson, On wood-water interactions in the over-hygroscopic moisture range: mechanisms, methods, and influence of wood modification, *Forests*, 2019, **10**, 779, doi: 10.3390/f10090779.
[29] W. Foudhil, P. Chen, K. Fahem, S. Harmand, S. Ben Jabrallah, Study of the evaporation kinetics of pure and binary droplets: volatility effect, *Heat and Mass Transfer*, 2021, **57**, 1773-1790, doi: 10.1007/s00231-021-03043-8.
[30] K. Chen, H. Zhang, U.-K. Ibrahim, W. Xue, H. Liu, A. Guo, The quantitative assessment of coke morphology based on the Raman spectroscopic characterization of serial petroleum cokes,

Fuel, 2019, **246**, 60-68, doi: 10.1016/j.fuel.2019.02.096.
[31] G. Rantitsch, A. Bhattacharyya, J. Schenk, N. K. Lünsdorf, Assessing the quality of metallurgical coke by Raman spectroscopy, *International Journal of Coal Geology*, 2014, **130**, 1-7, doi: 10.1016/j.coal.2014.05.005.
[32] Y. S. Zhang, R. E. Owen, P. R. Shearing, W. C. Maskell, D. J. L. Brett, G. Manos, A study of coke formed by heavy oil volatilization/decomposition on Y-zeolite, *Journal of Analytical and Applied Pyrolysis*, 2019, **141**, 104630, doi: 10.1016/j.jaap.2019.104630.
[33] X. Li, J. Hayashi, C. Li, FT-Raman spectroscopic study of the evolution of char structure during the pyrolysis of a Victorian brown coal, *Fuel*, 2006, **85**, 1700-1707, doi: 10.1016/j.fuel.2006.03.008.
[34] M. F. Vogt, J. H. Waller, R. D. Zabreznik, The problem of sulfur content in calcined petroleum coke, *JOM*, 1990, **42**, 33-35, doi: 10.1007/BF03221017.
[35] A. P. Nikitin, E. R. Khabibulina, E. S. Mikhaylova, N. V. Zhuravleva, Z. R. Ismagilov, Structural defects and the demineralization of Kuznetsk basin coal: data from Raman spectroscopy, *Coke and Chemistry*, 2019, **62**, 169-173, doi: 10.3103/s1068364x19050028.
[36] J. Y. An, J. B. Seo, J. H. Choi, J. H. Lee, H. Kim, Evaluation of characteristics of coke degradation after reaction in different conditions, *ISIJ International*, 2016, **56**, 226-232, doi: 10.2355/isijinternational.isijint-2015-482.
[37] V. M. Strakhov, Yield and quality of coke fractions from batch with a high content of gas coal, *Coke and Chemistry*, 2021, **64**, 18-26, doi: 10.3103/S1068364X21010075.
[38] P. Caputo, P. Calandra, V. Loise, M. Porto, A. Le Pera, A. A. Abe, B. Teltayev, M. L. Luprano, M. Alfè, V. Gargiulo, G. Ruoppolo, C. Oliviero Rossi, Physical chemistry supports circular economy: toward a viable use of products from the pyrolysis of a refuse-derived fuel and granulated scrap tire rubber as bitumen additives, *Eurasian Chemico-Technological Journal*, 2023, **25**, 173-181, doi: 10.18321/ectj1520.
[39] Q. Liu, S. Yang, C. Wang, Y. Ji, Effect of carbon solution-loss reaction on properties of coke in blast furnace, *Journal of Iron and Steel Research International*, 2020, **27**, 489-499, doi: 10.1007/s42243-020-00399-9.
[40] C. Ovalles, E. Rogel, P. Hajdu, T. Rea, K. Chaudhuri, K. Hench, D. Cuspard, M. E. Moir, Predicting coke morphology in Delayed Coking from feed characteristics, *Fuel*, 2020, **263**, 116739, doi: 10.1016/j.fuel.2019.116739.
[41] H. Zhang, H. Cheng, Q. Yang, Y. Ling, Z. Sun, L. Xiao, Optimization of the experimental conditions and calculation methods for determination of coke nanopores, *Coke and Chemistry*, 2021, **64**, 562-570, doi: 10.3103/S1068364X21120103.
[42] Y. Kawana, Reactivity of coke. II. effects of heat treatment of cokes on their specific surface areas and absolute specific reaction rates with carbon dioxide at 950 °C, *Bulletin of the Chemical Society of Japan*, 1954, **27**, 334-339, doi: 10.1246/bcsj.27.334.
[43] K. Toshtay, A. Auyezov, Z. Korkembay, S. Toktassynov, A. Seytkhan, A. Nurakyshev, Partial hydrogenation of sunflower oil on platinum catalysts: Influence of process conditions on the mass content of geometric isomers, *Molecular Catalysis*, 2021, **513**, 111819, doi: 10.1016/j.mcat.2021.111819.
[44] J. Xiao, F. Li, Q. Zhong, J. Huang, B. Wang, Y. Zhang, Effect of high-temperature pyrolysis on the structure and properties of coal and petroleum coke, *Journal of Analytical and Applied Pyrolysis*, 2016, **117,** 64-71, doi: 10.1016/j.jaap.2015.12.015.
[45] Z. Phua, A. Giannis, Z. Dong, G. Lisak, W. J. Ng, Characteristics of incineration ash for sustainable treatment and reutilization, *Environmental Science and Pollution Research*, 2019, **26**, 16974-16997, doi: 10.1007/s11356-019-05217-8.
[46] R. Javadli, A. de Klerk, Desulfurization of heavy oil, *Applied Petrochemical Research*, 2012, **1**, 3-19, doi: 10.1007/s13203-012-0006-6.
[47] S. Turganbay, S. B. Aidarova, N. E. Bekturganova, C. S. Li, K. B. Musabekov, S. S. Kumargalieva, K. Toshtay, Nanoparticles of sulfur as fungicidal products for agriculture, *Eurasian Chemico-Technological Journal*, 2012, **14**, 313-319, doi: 10.18321/ectj128.
[48] Y. Aubakirov, Z. Tashmukhambetova, Y. Imanbayev, N. Nurtazina, B. Kenzheyev, K. Toshtay, Comprehensive investigation of pyrolysis products from coal dust in southern Kazakhstan: An experimental study, *ES Materials & Manufacturing*, 2024, **24**, 1123, doi: 10.30919/esmm1123.